

Performance of window synchronisation in coherent optical ofdm system

Sofien Mhatli¹, Bechir Nsiri²

¹SERCOM, EPT

Université de Carthage, 2078, La Marsa, Tunis, Tunisia

²Sys'com Lab, ENIT, BP.37 Le Belvédère 1002

Tunis, Tunisia

Mutasam Jarajreh³, Basma Hammami², Rabah Attia¹

³Faculty of Engineering & Environment, Northumbria

University, Ellison Place, Newcastle upon Tyne, NE1

8ST, UK

Abstract—In this paper we investigate the performances of a robust and efficient technique for frame/symbol timing synchronization in coherent optical OFDM. It uses a preamble consisting of only two training symbol with two identical parts to achieve reliable synchronization schemes. The performances of the timing offset estimator at correct and incorrect timing in coherent optical OFDM are compared in term of mean and variance of the timing offset, and finally, we study the influence of number of subcarriers and chromatic dispersion.

Keywords—COFDM; timing offset; time synchronization; training symbol)

I. INTRODUCTION

Orthogonal frequency division multiplexing (OFDM) has been used in many telecommunication applications because of its high spectral efficiency and simple hardware implementation. OFDM has also been considered for optical systems as a candidate for future long range high data rate communication systems. The principle of frequency multiplexing is to group the digital data by N packets, which will be called OFDM symbol and modulating each given a different carrier simultaneously. One of the central features that set orthogonal frequency-division multiplexing (OFDM) apart from single-carrier modulation is its uniqueness of signal processing.

After transmission in fiber optic, the transmitted signal has distorted and rotated because the effect of white Gaussian noise (AWGN) and chromatic dispersion (CD) which are the reason why the system need channel estimation. For a high performances of the equalizer, we need have a precisely synchronization for the following module of channel estimator and channel equalizer.

T. Schmidl and D. Cox's algorithms make use of the correlation of training symbol to realize the synchronization. The synchronization algorithms depending on correlation need set a detect threshold of timing metric to detect whether the symbol synchronization succeed.

In this paper, we present the formulation of the Schmidl and Cox algorithm [4, 5] which is developed in radiofrequency, and we focus in depth on the performance of this algorithm in coherent optical OFDM. The rest of the article is organized as follows: in Section 2, the COFDM system is described. In section 3, the COFDM synchronization technique is described. The performance evaluation of synchronization system

presented and discussed in Section 4. Finally, Section 5 concludes the work.

II. COFDM SYSTEM DESCRIPTION

Figure 1 shows the conceptual diagram of a generic CO-OFDM system, including five basic functional blocks: RF OFDM transmitter, RF-to-optical (RTO) up-converter, optical link, optical-to-RF (OTR) down-converter, and RF OFDM receiver. In the RF OFDM transmitter, the input digital data are first converted from serial to parallel into a "block" of bits consisting of N_{sc} information symbol, each of which may comprise multiple bits for m-ary coding. This information symbol is mapped into a two-dimensional complex signal C_{ki} , for instance, using Gray coding, where C_{ki} stands for the mapped complex information symbol. The subscripts of C_{ki} correspond to the sequence of the subcarriers and OFDM blocks. The time domain OFDM signal is obtained through inverse discrete Fourier transform (IDFT) of C_{ki} , and a guard interval is inserted to avoid channel dispersion [6,7]. The resultant baseband time domain signal can be described as :

$$s_B(t) = \sum_{i=-\infty}^{+\infty} \sum_{k=-\frac{N_{sc}}{2}+1}^{k=N_{sc}/2} c_{ki} \Pi(t - Ts) e^{j2\pi f_k(t - iT_s)} \quad (1)$$

Where:

$$f_k = \frac{k-1}{t_s} \quad (2)$$

$$\Pi(t) = \begin{cases} 1, & (-\Delta G < t \leq t_s \\ 0, & t \leq -\Delta G, t > t_s \end{cases} \quad (3)$$

where C_{ki} is the i^{th} information symbol at the k^{th} subcarrier; f_k is the frequency of the k^{th} subcarrier; T_s is the number of OFDM subcarriers, ΔG , and t_s are the OFDM symbol period, guard interval length, and observation period, respectively; and $\Pi(t)$ is the rectangular pulse waveform of the OFDM symbol. The extension of the waveform in the time frame of $[-\Delta G, 0]$ in (1) represents the insertion of the cyclic prefix, or guard interval. The digital signal is then converted to an analog form through a DAC and filtered with a low-pass filter to remove the alias signal. The baseband OFDM signal can be further converted to an RF pass band through an RF IQ. The subsequent RTO up-converter transforms the base band signal to the optical domain using an optical IQ modulator comprising a pair of Mach-Zehnder modulators (MZMs) with

a 90 degree phase offset. The baseband OFDM signal is directly up-converted to the optical domain given by:

$$E(t) = e^{j(\omega_{LD1}t + \varphi_{LD1})} \cdot s_B(t) \quad (4)$$

Where ω_{LD1} and φ_{LD1} , respectively, are the angular frequency and phase of the transmitter laser. The up-converted signal $E(t)$ traverses the optical medium with an impulse response of $E'(t)$, and the received optical signal becomes:

$$E'(t) = e^{j(\omega_{LD1}t + \varphi_{LD1})} \cdot s_B(t) \otimes h(t) \quad (5)$$

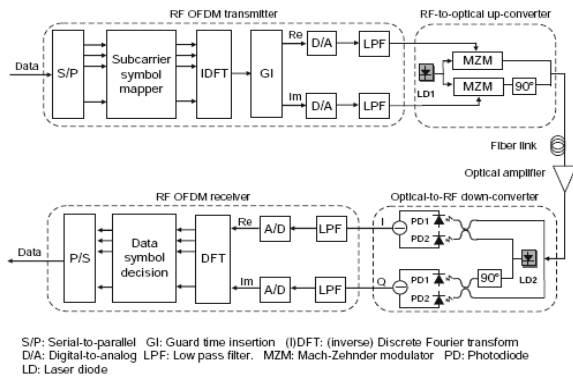


Fig. 1 Conceptual diagram for a generic CO-OFDM system with a direct up/down conversion architecture

Where \otimes stands for convolution. The optical OFDM signal is then fed into the OTR downconverter, where the optical OFDM signal is converted to an RF OFDM signal. The directly down-converted signal can be expressed as:

$$r(t) = e^{j(\omega_{off}t + \Delta\varphi)} \cdot r_0(t) \quad (6)$$

$$r_0(t) = s_B(t) \otimes h(t) \quad (7)$$

$$\omega_{off} = \omega_{LD1} - \omega_{LD2} \quad (8)$$

$$\Delta\varphi = \varphi_{LD1} - \varphi_{LD2} \quad (9)$$

$$c'_{ki} = e^{j\phi_i} e^{j\Phi_D(f_k)} T_k c_{ki} + n_i \quad (10)$$

$$\Phi_D(f_k) = \pi \cdot c \cdot D_r \cdot \frac{f_j^2}{f_0^2} \quad (11)$$

$$c'_{ki} = E'(t) \quad (12)$$

Where ω_{off} and $\Delta\varphi$ are respectively the angular frequency offset and phase offset between the transmitted and receive lasers. $\Phi_D(f_k)$ is the phase dispersion due to the fiber chromatic dispersion [8]. ϕ_i is the ofdm common phase error (CPE) [9] due to the phase noises from lasers and RF local oscillators at both the transmitter and receiver.

III. COFDM SYSTEM SYNCHRONISATION DESCRIPTION

In the RF OFDM receiver, the down-converted OFDM signal is first sampled with an ADC. Then the signal needs to go through the following three levels of sophisticated synchronizations before the symbol decision can be made:

- DFT window synchronization in which OFDM symbols are properly delineated to avoid intersymbol interference
- Frequency synchronization, namely frequency offset ω_{off} being estimated, compensated, and, preferably, adjusted to a small value at the start.
- The subcarrier recovery, where each subcarrier channel is estimated and compensated.

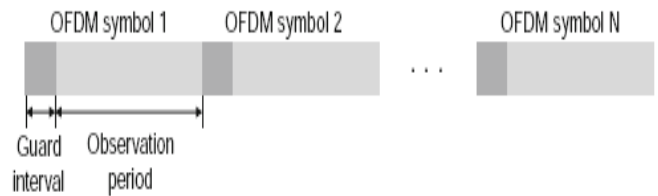


Fig. 2 Time domain structure of an OFDM signal

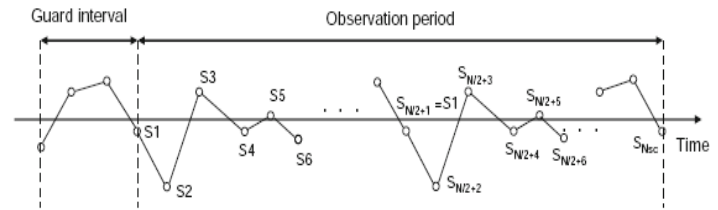


Fig. 3 the Schmidl synchronization format

Synchronization is one of the most critical functionalities for a CO-OFDM receiver. As discussed in the previous section, it can be divided into three levels of synchronization: DFT Window timing synchronization, carrier frequency offset synchronization, and subcarrier recovery. Figure 2 shows the time domain structure of an OFDM signal consisting of many OFDM symbols. Each OFDM symbol comprises a guard interval and an observation period. It is imperative that the start of the DFT window (i.e., the observation period) be determined properly because an improper DFT window will result in intersymbol interference (ISI) and intercarrier interference (ICI) [7].

One of the popular methods for window synchronization was proposed by Schmidl and Cox.[4]. In such a method, a pilot symbol or preamble is transmitted that consists of two identical segments, as shown in Figure 3, which can be expressed as:

$$s_m = s_{m-N_{sc}} \cdot m \in \left[\frac{N_{sc}}{2} + 1, N_{sc} \right] \quad (13)$$

Where s_m is the m th sample with a random value when m is from 1 to $N_{sc}/2$. Assuming a time-invariant channel impulse response function $h(t)$ the sampled received signal has the following form:

$$r_m = r\left(\frac{mt_s}{N_{sc}}\right) = r_m^0 e^{j(\omega_{off} \frac{mt_s}{N_{sc}})} + n_m \quad (14)$$

We have assumed that the constant phase across the entire OFDM symbol, or $\Delta\varphi$ equals zero in Eq. (9). The delineation can be identified by studying the following correlation function [4] defined as :

$$R(d) = \sum_{m=1}^{N_{sc}/2} r_{m+d}^* r_{m+d+N_{sc}/2} \quad (15)$$

The principle is based on the fact that the second half of r_m is identical to the first half except for a phase shift. Assuming the frequency offset ω_{off} is small to start with, we anticipate that when $d = 0$, the correlation function $R(d)$ reaches its maximum value. The correlation function can be normalized to its maximum value given by:

$$M(d) = \left| \frac{R_d}{S_d} \right| \quad (16)$$

And

$$S_d = \sqrt{\left(\sum_{m=1}^{N_{sc}/2} r_{m+d}^2 \right) \left(\sum_{m=1}^{N_{sc}/2} r_{m+d+N_{sc}/2}^2 \right)} \quad (17)$$

Where $M(d)$ is defined as the DFT window synchronization timing metric. The optimal timing metric has its peak at the correct starting point of the OFDM symbol that is:

$$d_{opt} = \arg\{\max [M(d)]\} \quad (18)$$

Where $\arg\{\max [M(d)]\}$ in general stands for searching the optimal argument of d that maximizes the objective function of $M(d)$, and d_{opt} stands for the optimal timing point.

IV. SIMULATION AND RESULT

We have conducted a matlab simulation for the coherent optical OFDM presented in figure 1 to confirm the DFT window synchronization using the Schmidl format for a CO-OFDM system at 10 Gb/s under the influence of chromatic dispersion, linewidth, and optical-to-signal noise ratio (OSNR).

TABLE I. SIMULATION PARAMETERS

Data rate (G/s)	10
Modulation	QAM
M	4
FFT Size	128
L(number of samples of the training symbol)	256
Number of samples per bit	4
Number of blocks	1
Number of symbols	100
Number of frames	100
CP length	1/8
Wavelength (nm)	1.55
Dispersion (ps/nm)	17000
Laser linewidth (KHz)	100

The OFDM system parameters used for the simulation are described in the TABLE I mentioned above.

A. Timing metric for CO-OFDM systems

This plot shows that the peak of the timing metric decreases from an ideal value of 1 to approximately 0.3 when the SNR is 0 dB. All curves show the flat platform corresponding to the guard interval inserted in the beginning of each symbol.

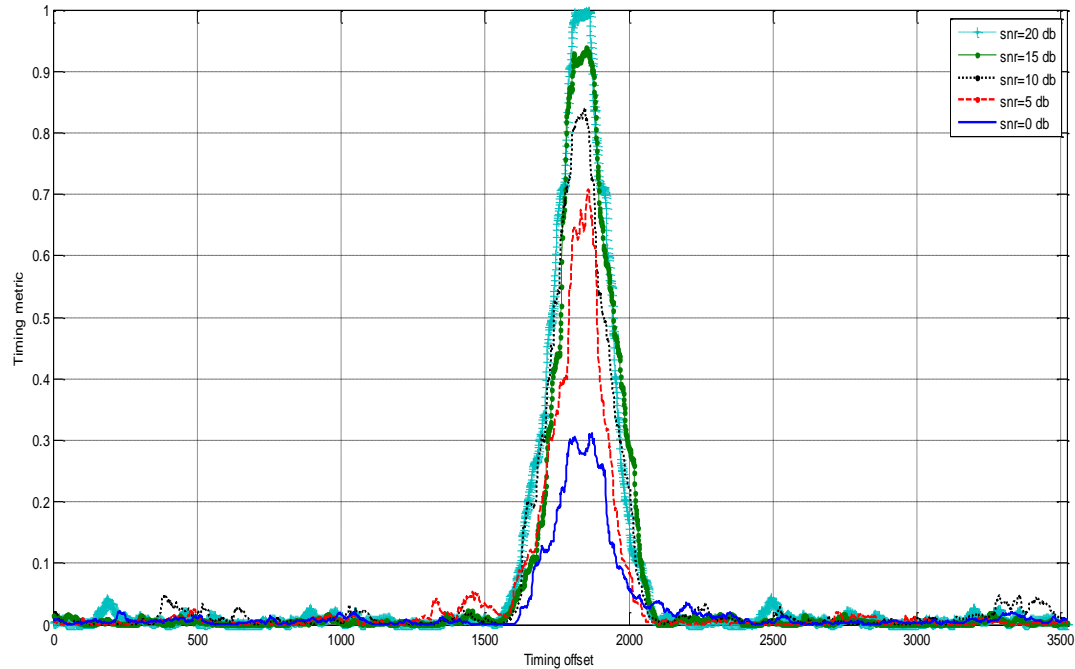


Fig. 4 Timing metric for CO-OFDM systems

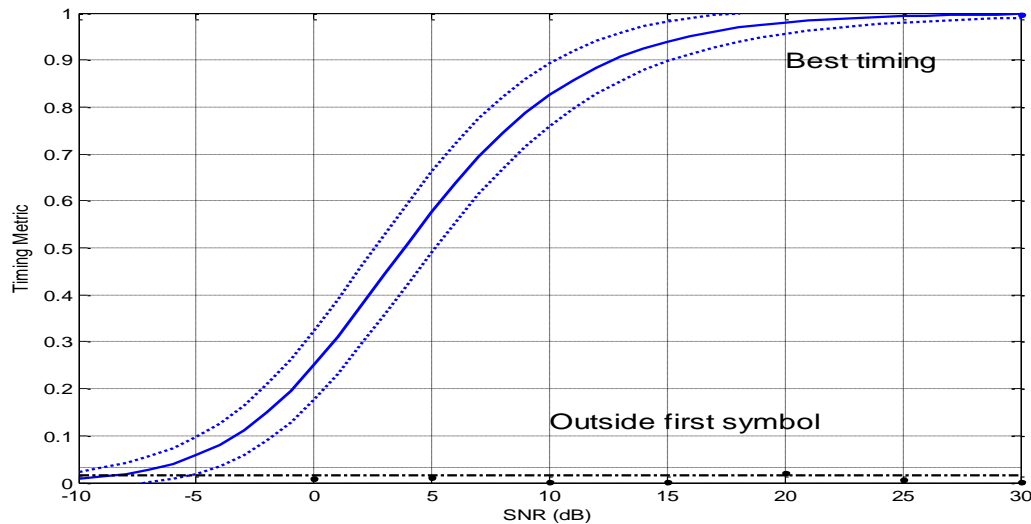


Fig. 5 Expected value of timing metric. (Dashed lines indicate three standard deviations)

This figure shows a plot of the expected value of timing metric $M(d)$ versus SNR at both the best timing instant and a point outside the training symbol. The dashed lines indicate three standard deviations from each curve.

We concluded that outside the training symbol the timing metric is null.

B. Mean and Variance at correct timing

The correct timing point was chosen at the start of the useful part of the first training symbol, the plots show that variance of timing metric is lower than the mean of timing metric.

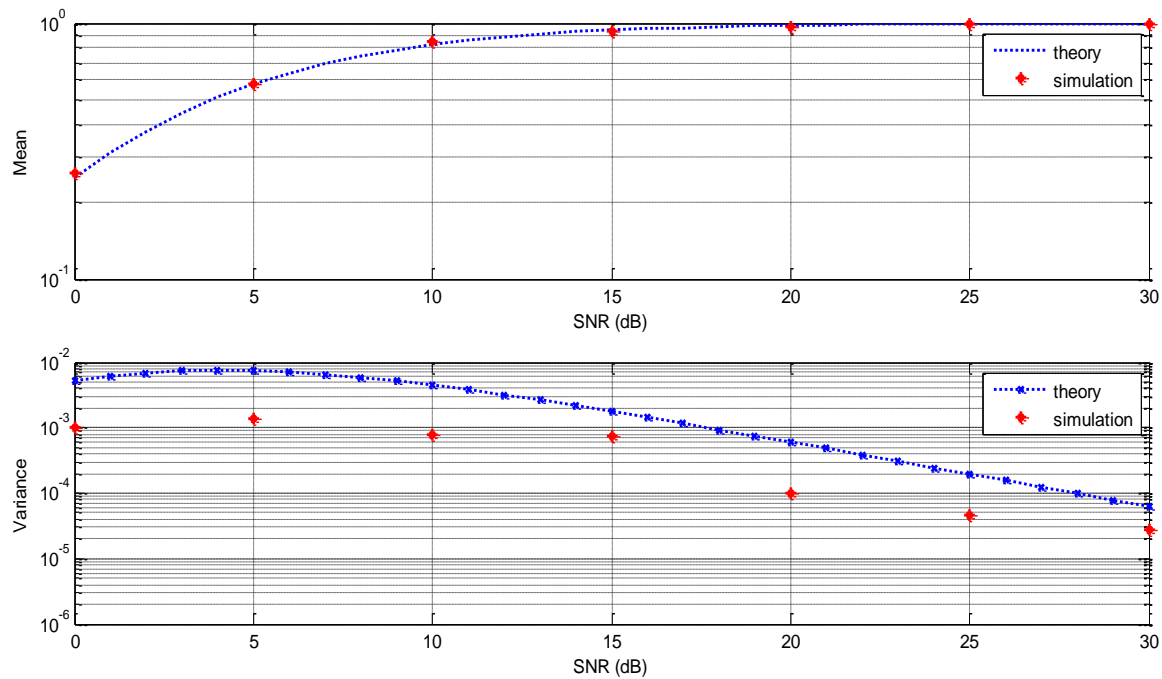


Fig. 6 Mean and Variance at correct timing

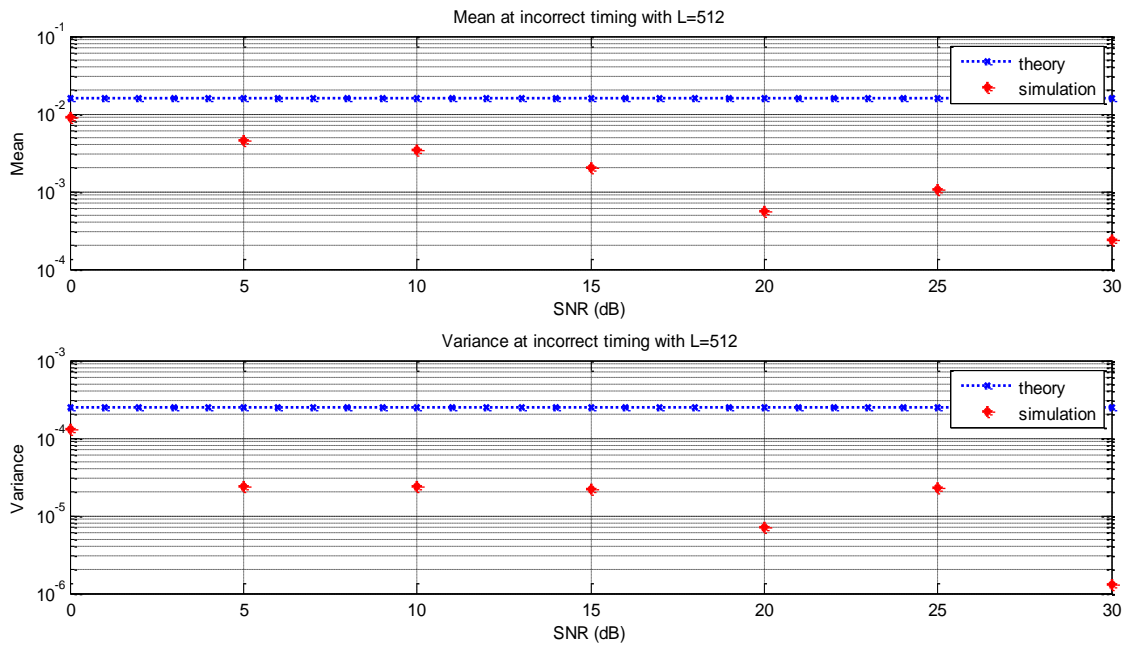


Fig. 7 Mean and variance at incorrect timing

Figure 6 shows the result of simulation for the correct timing.

C. Mean and Variance at incorrect timing

Figures 7 and 8 show the mean and variance of the incorrect timing. The incorrect timing point was chosen one symbol after the training symbol, the performance of the variance of timing metric is lower than the performance of the mean of the timing metric.

Some plot shows that there's a differentiation between the theory and simulation result and this lead on the two terms r_{m+d}^* and $r_{m+d+N_{sc}/2}$ which are dependent and we consider in the simulations that are independent.

D. Influence of chromatic dispersion

This plot show that the increase of the chromatic dispersion leads on an increase of the timing offset and the minimum timing offset correspond on a null chromatic dispersion.

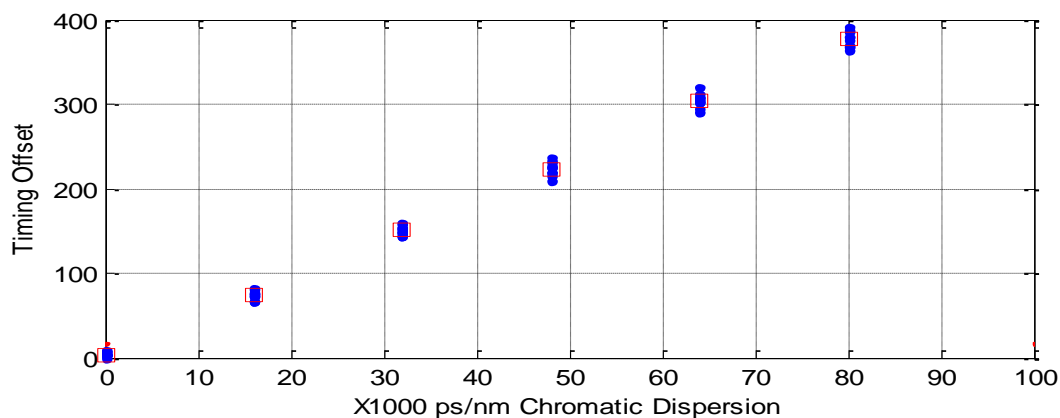


Fig. 8 Influence of chromatic dispersion

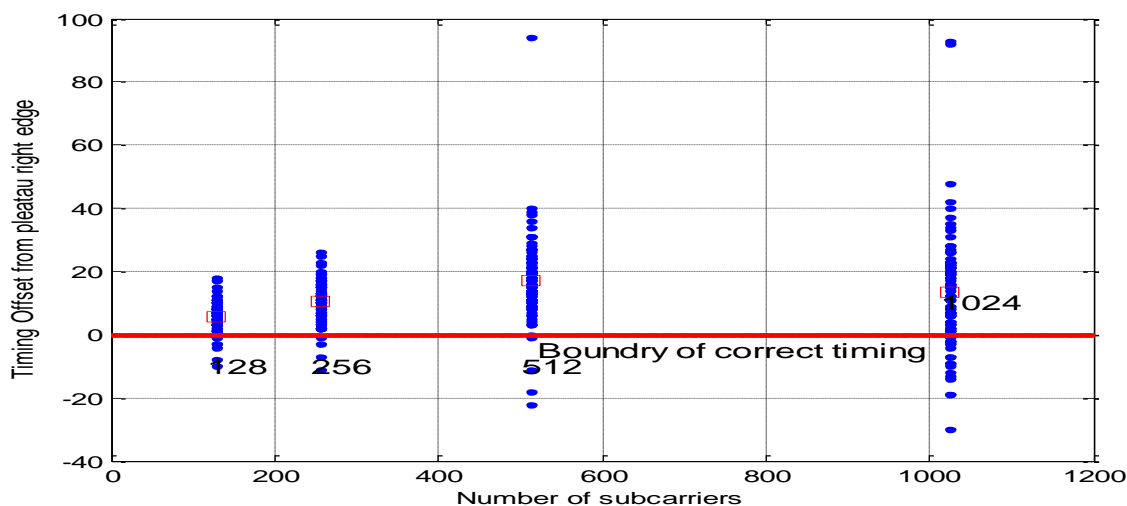


Fig. 9 Influence of number of subcarriers

E. Influence of number of subcarriers

This figure shows that the increase of the number of subcarrier lead on an increase of the timing offset; so to avoid this timing offset we must insert in the OFDM symbol in the beginning and in the end a sufficient number of zeros to avoid this increase of timing offset.

V. CONCLUSION

In this paper, we evaluated the performance of Schmidl and Cox algorithm of synchronization in coherent optical OFDM system. This method present a flat plateau in the timing offset versus SNR, so we aim in future works to eliminate this plateau and improve the performance of estimators in terms of mean and variance of timing metric and the complexity of synchronization algorithm.

REFERENCES

[1] Shieh.W and Authadage C. coherent optical orthogonal frequency division multiplexing; electronic letters.42(10),587–589 (2006).

[2] Shieh.W, Yang.Q, and MA.Y. 107 Gb/s coherent optical ofdm transmission over 1000km SSMF fiber using orthogonal band multiplexing, optics express,16(9),6378–6386 (2008).

[3] Ma CP, Kuo JW. Orthogonal frequency division multiplex with multi-level technology in optical storage application. Jpn J Appl Physics Part 1: Regular Papers Short Notes Rev Papers 2004;43:4876–8.

[4] Schmidl TM, Cox DC. Robust frequency and timing synchronization for OFDM. IEEE Trans Commun 1997;45:1613–21.

[5] Minn H, Bhargava VK, Letaief KB. A robust timing and frequency synchronization for OFDM systems. IEEE Trans Wireless Commun 2003;2:822–39.

[6] Hara S, Prasad R. Multicarrier Techniques for 4G Mobile Communications. Boston: Artech House; 2003.

[7] Hanzo L, Munster M, Choi BJ, Keller T. OFDM and MC-CDMA for Broadband Multi-User Communications, WLANs and Broadcasting. New York: Wiley; 2003.

[8] Bauml RW, Fischer RFH, Huber JB. Reducing the peak-to-average power ratio of multicarrier modulation by selected mapping. IET Electron Lett 1996;32:2056–7.

[9] Friese M. OFDM signals with low crest-factor. In: Proc. 1997 IEEE Global Telecommun. Conf; 1997. pp. 290–4.